Nanostructured Materials and Nanotechnology IV

Ceramic Engineering and Science Proceedings
Volume 31, Issue 7, 2010

Edited by
Sanjay Mathur
Suprakas Sinha Ray

Volume Editors
Sanjay Mathur
Tatsuki Ohji

WILEY

The American Ceramic Society

Nanostructured Materials and Nanotechnology IV

A Collection of Papers Presented at the 34th International Conference on Advanced Ceramics and Composites January 24–29, 2010 Daytona Beach, Florida

Edited by
Sanjay Mathur
Suprakas Sinha Ray

Volume Editors
Sanjay Mathur
Tatsuki Ohji

The American Ceramic Society

WILEY

A John Wiley & Sons, Inc., Publication

Published by John Wiley & Sons, Inc., Hoboken, New Jersey.
Published simultaneously in Canada.

Library of Congress Cataloging-in-Publication Data is available.

ISBN 978-0-470-59472-8

Printed in the United States of America.

10 9 8 7 6 5 4 3 2 1

Nanostructured Materials and Nanotechnology IV

Preface

The 4th International Symposium on Nanostructured Materials and Nanotechnology was held during the 34th International Conference and Exposition on Advanced Ceramics and Composites, in Daytona Beach, Florida during January 24–29, 2010. This symposium provided, for the fourth consecutive year, an international forum for scientists, engineers, and technologists to discuss new developments in the field of nanotechnology. This year's symposium had a special focus on the large-scale production and potential of nanomaterials in energy applications. The symposium covered a broad perspective including synthesis, processing, modeling and structure-property correlations in Nanomaterials and nanocomposites. More than 90 contributions (invited talks, oral presentations, and posters) were presented by participants from universities, research institutions, and industry, which offered interdisciplinary discussions indicating strong scientific and technological interest in the field of nanostructured systems. The geographical spread of the symposium was impressive with participants coming from 16 nations.

This issue contains 17 peer-reviewed (invited and contributed) papers covering various aspects and the latest developments related to processing, modeling and manufacturing technologies of nanoscaled materials including inorganic-organic nanocomposites, nanowire-based sensors, new generation photovoltaic cells, self-assembly of nanostructures, functional nanostructures for cell tracking and heterostructures. Each manuscript was peer-reviewed using The American Ceramic Society review process.

The editors wish to extend their gratitude and appreciation to all the authors for their cooperation and contributions, to all the participants and session chairs for their time and efforts, and to all the reviewers for their valuable comments and suggestions. Financial support from the Engineering Ceramic Division of The American Ceramic Society is gratefully acknowledged. The invaluable assistance of the ACerS's staff of the meetings and publication departments, instrumental in the success of the symposium, is gratefully acknowledged,

We believe that this issue will serve as a useful reference for the researchers and

technologists interested in science and technology of nanostructured materials and devices.

SANJAY MATHUR
University of Cologne
Cologne, Germany

SUPRAKAS SINHA RAY
National Centre for Nano Structured Materials
CSIR, Pretoria, South Africa

Introduction

This CESP issue represents papers that were submitted and approved for the proceedings of the 34th International Conference on Advanced Ceramics and Composites (ICACC), held January 24–29, 2010 in Daytona Beach, Florida. ICACC is the most prominent international meeting in the area of advanced structural, functional, and nanoscopic ceramics, composites, and other emerging ceramic materials and technologies. This prestigious conference has been organized by The American Ceramic Society's (ACerS) Engineering Ceramics Division (ECD) since 1977.

The conference was organized into the following symposia and focused sessions:

Symposium 1	Mechanical Behavior and Performance of Ceramics and Composites
Symposium 2	Advanced Ceramic Coatings for Structural, Environmental, and Functional Applications
Symposium 3	7th International Symposium on Solid Oxide Fuel Cells (SOFC): Materials, Science, and Technology
Symposium 4	Armor Ceramics
Symposium 5	Next Generation Bioceramics
Symposium 6	International Symposium on Ceramics for Electric Energy Generation, Storage, and Distribution
Symposium 7	4th International Symposium on Nanostructured Materials and Nanocomposites: Development and Applications
Symposium 8	4th International Symposium on Advanced Processing and Manufacturing Technologies (APMT) for Structural and Multifunctional Materials and Systems
Symposium 9	Porous Ceramics: Novel Developments and Applications
Symposium 10	Thermal Management Materials and Technologies
Symposium 11	Advanced Sensor Technology, Developments and Applications

Focused Session 1	Geopolymers and other Inorganic Polymers
Focused Session 2	Global Mineral Resources for Strategic and Emerging Technologies
Focused Session 3	Computational Design, Modeling, Simulation and Characterization of Ceramics and Composites
Focused Session 4	Nanolaminated Ternary Carbides and Nitrides (MAX Phases)

The conference proceedings are published into 9 issues of the 2010 Ceramic Engineering and Science Proceedings (CESP); Volume 31, Issues 2–10, 2010 as outlined below:

- Mechanical Properties and Performance of Engineering Ceramics and Composites V, CESP Volume 31, Issue 2 (includes papers from Symposium 1)
- Advanced Ceramic Coatings and Interfaces V, Volume 31, Issue 3 (includes papers from Symposium 2)
- Advances in Solid Oxide Fuel Cells VI, CESP Volume 31, Issue 4 (includes papers from Symposium 3)
- Advances in Ceramic Armor VI, CESP Volume 31, Issue 5 (includes papers from Symposium 4)
- Advances in Bioceramics and Porous Ceramics III, CESP Volume 31, Issue 6 (includes papers from Symposia 5 and 9)
- Nanostructured Materials and Nanotechnology IV, CESP Volume 31, Issue 7 (includes papers from Symposium 7)
- Advanced Processing and Manufacturing Technologies for Structural and Multifunctional Materials IV, CESP Volume 31, Issue 8 (includes papers from Symposium 8)
- Advanced Materials for Sustainable Developments, CESP Volume 31, Issue 9 (includes papers from Symposia 6, 10, and 11)
- Strategic Materials and Computational Design, CESP Volume 31, Issue 10 (includes papers from Focused Sessions 1, 3 and 4)

The organization of the Daytona Beach meeting and the publication of these proceedings were possible thanks to the professional staff of ACerS and the tireless dedication of many ECD members. We would especially like to express our sincere thanks to the symposia organizers, session chairs, presenters and conference attendees, for their efforts and enthusiastic participation in the vibrant and cutting-edge conference.

ACerS and the ECD invite you to attend the 35th International Conference on Advanced Ceramics and Composites (http://www.ceramics.org/icacc-11) January 23–28, 2011 in Daytona Beach, Florida.

Sanjay Mathur and Tatsuki Ohji, Volume Editors
July 2010

Contents

CORE - SHELL NANOSTRUCTURES: SCALABLE, ONE-STEP AEROSOL SYNTHESIS AND IN-SITU SiO_2 COATING AND FUNCTIONALIZATION OF TiO_2 AND Fe_2O_3 NANOPARTICLES

J.T.N. Knijnenburg, A. Teleki, B. Buesser, S.E. Pratsinis
Particle Technology Laboratory, Institute of Process Engineering
Department of Mechanical and Process Engineering
Swiss Federal Institute of Technology, ETH Zurich
Sonneggstrasse 3, CH-8092 Zurich, Switzerland

ABSTRACT

Scalable flame aerosol synthesis of surface-functionalized and coated nanoparticles in one-step is presented. These composite materials provide the functionality of nanoparticles and even "cure" any deleterious effects that might have. So they can be incorporated readily in a liquid or polymer matrix. Magnetic maghemite core nanoparticles are made by a spray flame and coated in-situ by judiciously positioning (as guided by computational fluid dynamics simulations) a hollow ring that delivers in swirling mode precursor coating vapor for the SiO_2 shell through 1 to 16 jets. This results in hermetically-coated superparamagnetic particles (15-20 nm) with a 1-3 nm thin silica film as determined by microscopy and thermal conductivity measurements. Furthermore, the extent of surface functionalization by organic coatings is evaluated by infrared spectroscopy and dynamic light scattering of particle suspensions in organic solvents.

INTRODUCTION

The need for coating or surface modification of nanostructured particles comes from the fact that typically the surface properties of as-prepared particles are different than the desired ones for the final applications. In such systems, the core particle possesses functionality while the shell enhances or facilitates the interaction with the host liquid or solid matrix. A classic example of functional core particles is the coating of TiO_2 pigment particles with SiO_2. Light scattering by the TiO_2 core gives the desired white color whereas the SiO_2 shell allows incorporating the particles in paints or polymers by blocking the reactivity of TiO_2 which would otherwise degrade the surrounding material.[1] In other applications (e.g. V_2O_5-TiO_2 catalysts) the core provides the support (TiO_2) of the catalytically active V_2O_5 for deNOx selective catalytic reduction[2] or for synthesis of phthalic anhydride.[3]

Also magnetic nanoparticles can bind to drugs and proteins that can be guided in the human body using external magnetic fields.[4] Although metal oxides have a lower magnetization than metallic nanoparticles, the latter are highly reactive and toxic and therefore less suitable for biomedical applications.[5] Iron oxide nanoparticles have been widely investigated for in vivo applications (e.g. magnetic resonance imaging (MRI) contrast enhancement and drug delivery).[4,5] Such magnetic iron oxide nanoparticles are frequently coated with silica to improve their functionality and biocompatibility.[5] The silica coating makes the nanoparticles stable in aqueous conditions and limits magnetically induced self-agglomeration of magnetic cores. Furthermore, the silanol groups on the silica surface are able to react further with alcohols and silanes to make stable nonaqueous suspensions and can be further modified by covalent bonding of specific ligands.[4] Moreover, silica-coated or -embedded maghemite (γ-Fe_2O_3) nanoparticles exhibit improved thermal stability. Pure or uncoated γ-Fe_2O_3 is thermally unstable and is transformed to hematite (α-Fe_2O_3), the most stable form at high temperatures.[6] Silica inhibits such transformations of γ-Fe_2O_3 in O_2 or in air.[7,8] Various studies have been done on the incorporation of Fe_xO_y nanoparticles in polymers to obtain superparamagnetic, transparent nanocomposites.[9,10] Coating maghemite with silica facilitates homogeneous distribution of nanoparticles in a polymer matrix.[11] Typically such coatings are made by a sol-gel process[7,12] involving several steps, as Fe_xO_y core formation and its SiO_2 coating are two separate unit operations.

Nanocomposites combine the advantages of the inorganic filler material (e.g. thermal stability, rigidity) and the organic host polymer (e.g. flexibility, processability), having enhanced electrical, optical or mechanical properties over the individual components.[13,14] Surface functionalization of hydrophilic nanoparticles increases their hydrophobicity and can also include reactive groups (e.g. vinyl groups) that can cause further crosslinking between particles and host polymer.[14] For example, silica dispersibility into an acrylic-based polyurethane is improved by surface functionalization of hydrophilic silica with long chain coupling agents like octyltriethoxysilane (OTES) while the non-functionalized silica showed inhomogeneous dispersion that reduces strength and transparency of the nanocomposite.[15]

Wet phase functionalization of flame-made particles has been studied in some detail. For example, flame-made radiopaque[16] and amorphous Ta_2O_5/SiO_2 nanoparticles were functionalized[17] and subsequently incorporated into a polyacrylate matrix.[16,18] Functionalization of these powders facilitated dispersion into the polymer matrix.[18]

Particle suspensions are generally sterically stabilized with an organic adlayer that acts as a steric barrier counteracting the attractive forces causing agglomeration.[19] Long shelf-life suspensions have direct applications as electronic ink displays, where the image quality is affected by the uniformity and stability of particle dispersions inside an organic medium.[20,21] Dilute suspensions are used for biomedical applications,[4,5] while the more concentrated ones (30-40 vol%) find their application in further processing into organic films on devices (i.e. sensors or solar cells) by screen-printing or tape casting.[22,23]

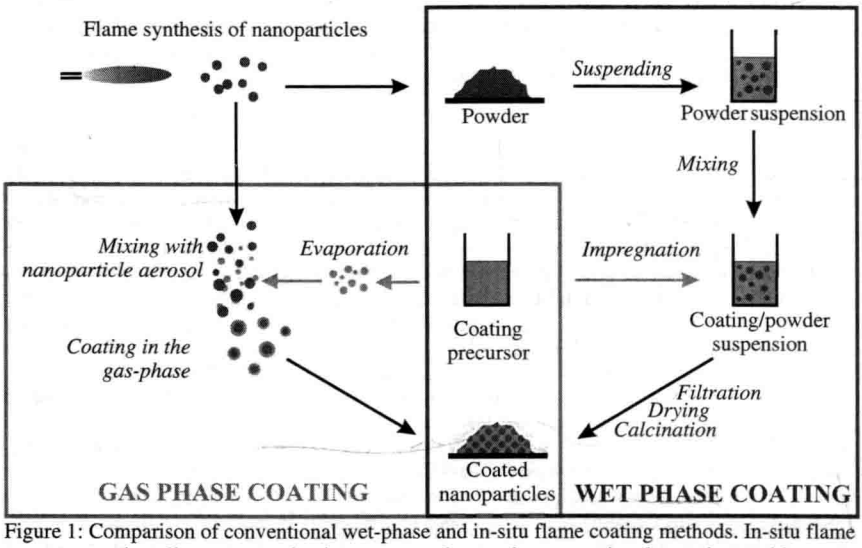

Figure 1: Comparison of conventional wet-phase and in-situ flame coating methods. In-situ flame coating allows preparation in one step, whereas the conventional route is a multi-step process.

Typically[3] surface functionalization processes have multiple steps (ex-situ synthesis) where the core material is formed first, followed by a second operation where coating is done (Figure 1: wet phase coating).[24] In-situ processes are available as well in the wet phase, where the coating is done at

the same time as core particle is formed.[15,24,25] There is, however, an increasing interest in rapid gas phase processes. Aerosol routes are attractive as they offer fewer process steps than conventional wet chemistry, easier particle collection from gaseous rather than liquid streams and no liquid by-products that require costly cleaning.[26] In addition, aerosol-made particles and films have unique morphology and high purity (e.g. optical fibers) and sometimes even metastable phases[27] (e.g. low temperature $BaCO_3$ for NOx storage-reduction or ε-WO_3 for ultraselective sensing of acetone, a tracer of diabetes[28]) leading to synthesis of mixed oxides, metal salts and pure metals as well as layered particles and solid or highly porous films with unique functionality resulting in novel catalysts, micropatterned sensors, phosphors, battery, solar and fuel cell electrodes, dental prosthetics, nutritional supplements[27] and even durable sorbents for CO_2 sequestration.[29]

Many metal oxides (e.g. TiO_2, SiO_2) are made today on a large scale in flame aerosol reactors. However for the coating of these products often costly and extensive wet-phase processes are required. In fact, the cost of coating pigmentary TiO_2 particles is comparable to their coating and functionalization cost.[30] As a result, there is a need for continuous gas phase coating or functionalization processes and in particular to simplify and improve such processes by combining both particle synthesis and coating in a one-step gas phase process (Figure 1: gas phase coating). Coherent and homogeneous coating on all particles is essential for optimal performance. A "coherent coating" in this context means that the core particle and the coating material stick (cohere) together. A "homogeneous coating" signifies that the coating has the same thickness around the core particle, i.e. the silica is distributed evenly over the core surface without any "patches". Furthermore, optimization of coating thickness is desired, as silica decreases the UV absorbance of TiO_2 (e.g. in sunscreens) and increases production costs. Scalable production of pure[31] and mixed oxides[32] up to 1 kg/h can be achieved using flame spray aerosol processes even in academic laboratories. At industrial facilities this is in the order of 25 tons/h.

IN-SITU COATING OF FLAME-MADE TITANIA

An alternative process for the scalable manufacture of silica-coated nanoparticles in one step is flame spray pyrolysis (FSP).[33-35] Various studies have been performed on coating of freshly-made TiO_2 with silica. Teleki et al.[34] coated rutile TiO_2 particles by injection of hexamethyldisiloxane (HMDSO), a Si precursor, downstream of the TiO_2 formation zone in an enclosed FSP reactor. Figure 2a shows the experimental setup, where the FSP reactor is enclosed by a 5-30 cm long quartz glass tube (4.5 cm ID).

There Al-doped (4 wt% Al_2O_3) rutile TiO_2 particles were produced by FSP of a 1 M solution of aluminum sec-butoxide and titanium-tetra-isopropoxide in xylene. The precursor solution was injected through the inner capillary with a flow rate of 5 mL/min, dispersed with 5 L/min O_2 (pressure drop 1.5 bar) and sheathed by another 40 L/min O_2. The solution spray was ignited by a ring shaped methane/oxygen (1.5/3.2 L/min) premixed flame.[33,36] At the top of the lower glass tube, a stainless steel metal torus pipe (0.38 cm ID) ring (4.5 cm ID) with 1, 2, 4, 8 or 16 radial outlets (0.06 cm each in diameter) was placed. The outlets are directed 10° away from the ring radius and pointed 20° downstream[37] to enable judicious swirl mixing of the coating precursor vapor with the titania-containing aerosol stream. Above the ring, another 30 cm long quartz glass tube (4.5 cm ID) was placed. Through the torus ring outlets, a gas flow of 0.8 L/min N_2 carrying HMDSO vapor (the Si coating precursor) was injected with an additional 15 L/min N_2. The product particles are collected on a glass fiber filter using a vacuum pump.

The effect of burner-ring-distance (BRD) on the coating quality was determined experimentally.[34] Injection of HMDSO vapor at low BRD (where high temperature and TiO_2 formation still takes place) leads to fast oxidation of HMDSO, resulting in separate SiO_2 and TiO_2 particles or domains. In contrast, all particles were coated homogeneously with 2-3 nm thick SiO_2 films and no

separate domains or particles were obtained when HMDSO was injected at BRD ≥ 20 cm. The coating quality was verified by photooxidation of isopropyl alcohol (IPA).[38] Titania is photocatalytically active converting IPA to acetone. So the released acetone concentration by photooxidation of IPA slurries containing SiO_2-coated TiO_2 made at various BRD was determined by gas conductivity measurements. This confirmed the formation of hermetic SiO_2 coatings onto the TiO_2 particles.[35]

The influence of silica content on the coating morphology was studied at a BRD of 20 cm.[34] For 5 wt% SiO_2 no coating film was visible by TEM due to the low theoretical coating thickness (< 1 nm for a 40 nm particle). The existence of such SiO_2 shells was confirmed[34] as it had reduced the photooxidation of IPA to acetone to 50%. Increasing to 10 or 20 wt% SiO_2 yielded homogeneous hermetic coatings of 2-4 nm thick in agreement with the expected theoretical coating thickness. For these concentrations, no separate silica particles were observed by TEM while the quality of the coating was confirmed by photocatalytic evaluation of such particle slurries containing IPA.

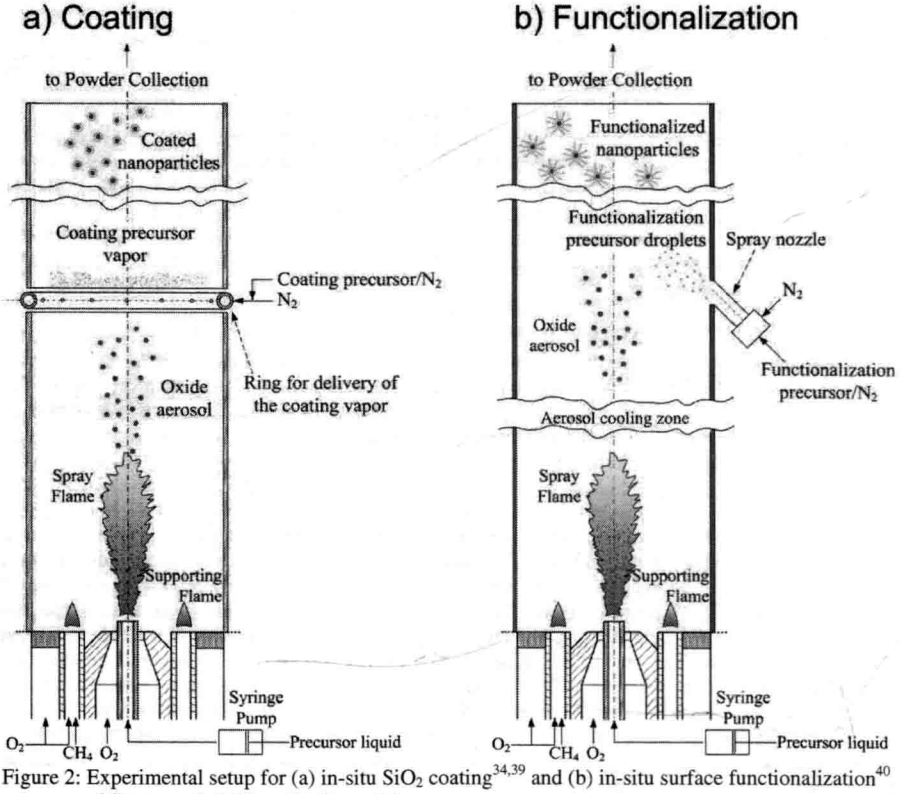

Figure 2: Experimental setup for (a) in-situ SiO_2 coating[34,39] and (b) in-situ surface functionalization[40] of flame-made TiO_2 or Fe_2O_3 particles.

The mixing of aerosol with vapor during TiO_2 coating by SiO_2 was studied also by varying N_2 flow rate and the number of coating jets. Such coating was optimized by systematic design using computational fluid dynamics (CFD) where the mixing of the incoming HDMSO-containing N_2 flow

with the product TiO_2 aerosol was visualized. The volume fraction of the carrier N_2 in the stream is an indication for the mixing efficiency of HMDSO as N_2 is the main component of the coating precursor stream. Figure 3 shows the N_2 volume fraction distribution along the tube axis above the ring for various N_2 volume flow rates. The flows at the jet outlets are red as they contain 100 vol% N_2. At a low overall jet flow rate of 5 L/min (Figure 3a) the N_2 flow remains largely near the tube wall while N_2-poor regions remain along the centerline of the tube. Increasing the flow rate to 10 L/min (Figure 3b) improves homogeneity along and across the tube, however still rather limited mixing of the HMDSO-laden vapor stream with the TiO_2 particle-containing aerosol takes place. For high flow rates (15 L/min), some N_2 lean regions (blue) are still present above the torus ring along the reactor walls by the high jet exit velocity,[33] but there is already improved mixing at 3 cm above the injection point, shown by the rather homogeneous concentration of 15-30 vol% N_2 (green). With increasing height above the torus ring, however, the flow becomes more homogeneous throughout the tube,[33] in stark contrast to the lower jet flow rates (Figure 3a,b).

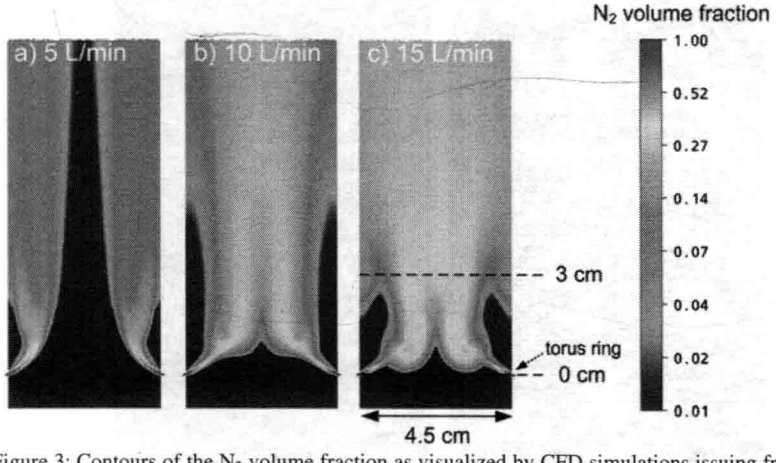

Figure 3: Contours of the N_2 volume fraction as visualized by CFD simulations issuing from 16 jets of a torus ring[34] with a volume flow of 5 (a), 10 (b) and 15 L/min N_2 (c, adopted from Teleki et al.[33]). The logarithmic color scale ranges from < 0.01 (blue) to 1 (red) N_2.

The homogeneity of the SiO_2 coating on the rutile TiO_2 nanoparticles was verified experimentally at different HMDSO-laden N_2 injection flow rates: Figure 4 displays TEM images of rutile TiO_2 nanoparticles coated with 20 wt% SiO_2 at various N_2 flow rates. At 5 (Figure 4a) and 10 (Figure 4b) L/min, the coating is rather inhomogeneous and large domains of separate amorphous SiO_2 particles are clearly visible. For 20 (Figure 4c) and 30 (Figure 4d) L/min N_2, all titania particles appear to be coated without any separate SiO_2 particles. This is attributed to the improved mixing and the decreased silica precursor concentration which forms smaller silica particles that can deposit and sinter faster on the titania rather than collide with other SiO_2 coating particles and form larger ones. As a result, smooth coating films are formed.

Teleki et al.[33] have visualized by CFD the effect of the number of jets issuing from the torus pipe. This plays a large role in the homogeneity of the flow. For increasing number of jet outlets, the N_2 concentration is more homogeneous and the mixing quality increases. For only 1 jet, the N_2 concentration was enriched at the walls opposite of the coating precursor inlet. With 2 or 4 inlets still

poorly mixed regions exist, while with 16 jets the concentration profile is uniform over the tube radius. These results were verified also experimentally: Separate silica domains as well as uncoated and homogeneously SiO_2-coated TiO_2 particles were observed with 1 and 4 inlets with low N_2 flows; for 8 inlets, at low injection velocity still separate silica is observed, however increasing the flow rate has shown to improve the coating quality and efficiency.

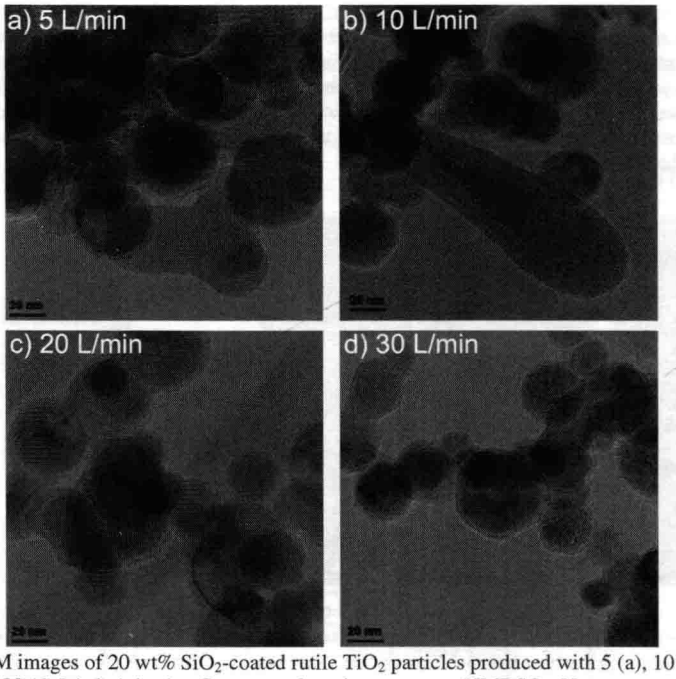

Figure 4: TEM images of 20 wt% SiO_2-coated rutile TiO_2 particles produced with 5 (a), 10 (b), 20 (c) and 30 (d) L/min injection flow rate of coating precursor HMDSO - N_2 stream.

SILICA COATING OF SUPERPARAMAGNETIC IRON OXIDE NANOPARTICLES

The potential of the above process involving sequential core oxide particle formation followed by coating it with nanothin silica layer is explored in synthesis of iron oxide - silica core shell nanoparticles. So, silica-coated γ-Fe_2O_3 nanoparticles were also made in one step using an enclosed FSP reactor.[39] In this process, the precursor consists of iron(III)acetylacetonate ($Fe(acac)_3$) dissolved in xylene/acetylene (3:1 in volume) to form a 0.34 M solution. The freshly formed Fe_2O_3 nanoparticle aerosol is mixed downstream with HMDSO vapor (Figure 2a).

Figure 5 displays images of pure (a) and SiO_2-coated (b-d) γ-Fe_2O_3 nanoparticles. The uncoated maghemite particles are pure, mostly hexagonally-shaped crystals as typically observed with flame-made iron oxide nanoparticles.[41] At 6.5 wt% SiO_2 coating (Figure 5b) no clear silica layer around the iron oxide could be observed. This concentration would correspond to a theoretical coating thickness of < 1 nm. At 17 (Figure 5c) and 23 wt% SiO_2 (Figure 5d) a homogeneous amorphous film of around 2 nm thick on the γ-Fe_2O_3 nanoparticles is formed. The latter particles are similar to those obtained by

sol-gel coating of maghemite with 43 wt % SiO_2.[42] No clear difference in aggregation or agglomeration can be distinguished between the uncoated and coated Fe_2O_3 particles. As confirmed by dynamic light scattering measurements,[39] the SiO_2-coated Fe_2O_3 particles exhibited excellent dispersibility in water compared to that of flame-made co-oxidized SiO_2/Fe_2O_3 and uncoated Fe_2O_3. The presence of the silica coatings decreases the isoelectric point of aqueous suspensions of such nanoparticles from around pH 7 for uncoated Fe_2O_3 to around pH 1.7 for 23 wt% SiO_2-coated Fe_2O_3, thereby inhibiting their magnetically-induced self-agglomeration.[39]

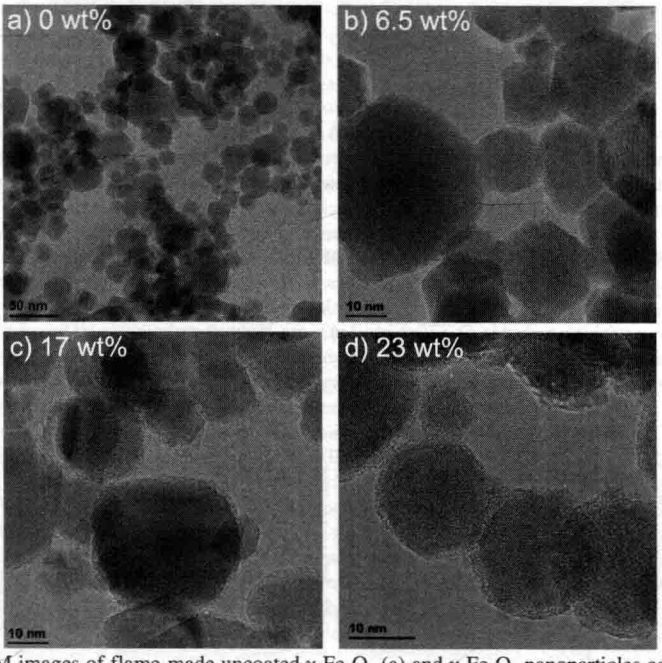

Figure 5: TEM images of flame-made uncoated γ-Fe_2O_3 (a) and γ-Fe_2O_3 nanoparticles coated with 6.5 wt% (b), 17 wt% (c) and 23 wt% (d) SiO_2 by injection of HMDSO vapor.

To compare, mixed SiO_2/Fe_2O_3 particles were also made by FSP of xylene/acetonitrile (75/25 by volume) solutions containing both HMDSO and $Fe(acac)_3$ in the enclosed reactor. In such SiO_2/Fe_2O_3 particles containing 36 (Figure 6a) and 46 wt% SiO_2 (Figure 6b), crystalline iron oxide particles are segregated to the edge of amorphous SiO_2 particles,[42] in contrast to the SiO_2-coated Fe_2O_3 made by introducing the Si-precursor downstream of the Fe_xO_y formation (e.g. Figure 5c,d).

The magnetic properties of the SiO_2-coated γ-Fe_2O_3 nanoparticles were measured by a vibrating sample magnetometer. The powders showed near zero hysteresis and were found to have a slightly lower magnetization than that of pure γ-Fe_2O_3. Their magnetization however was superior to that of co-oxidized SiO_2/Fe_2O_3 and commercial MagSilica. This means that SiO_2-coated γ-Fe_2O_3 nanoparticles retain most of the magnetic properties of Fe_2O_3.